Reformulation of the nonlocal coherent-potential approximation as a unique reciprocal-space theory of disorder

D. A. Rowlands,[1] X.-G. Zhang,[2,3] and A. Gonis[1]
[1]*Chemistry, Materials, Earth and Life Sciences, Lawrence Livermore National Laboratory, P.O. Box 808, L-367, Livermore, California 94551, USA*
[2]*Center for Nanophase Materials Sciences, Oak Ridge National Laboratory, Oak Ridge, Tennessee 37831-6493, USA*
[3]*Computer Science and Mathematics Division, Oak Ridge National Laboratory, Oak Ridge, Tennessee 37831-6493, USA*
(Received 7 July 2008; published 25 September 2008)

The nonlocal coherent-potential approximation (NLCPA) has recently been introduced for describing short-range correlations in disordered systems, and has been used to study short-range-ordering effects in alloys. However, it has recently been shown to yield spurious and nonunique results for small cluster sizes used in the calculation (with such features gradually disappearing as the cluster size increases). In this paper we reformulate the NLCPA as a unique and systematic theory. The formalism is based upon averaging the (phase-dependent) Green's function over all possible choices of phase. As a consequence, a fully continuous self-energy and spectral function are obtained for all cluster sizes. We show that the previous formalism is a specific limiting case of the reformulation, and explicitly demonstrate the theory for a one-dimensional tight-binding model in order to compare with exact numerical results.

DOI: 10.1103/PhysRevB.78.115119 PACS number(s): 71.15.−m, 71.23.−k, 71.20.−b, 71.27.+a

I. INTRODUCTION

Substitutionally disordered systems are comprised of a random distribution of N sites over a lattice, each of which can be of a different type α with the corresponding probabilities of occupation or concentrations c_α summing to unity, i.e., $\Sigma_\alpha c_\alpha = 1$. For example, a disordered binary alloy consists of sites which can be of chemical type $\alpha = A$ or B. Because an exact average over all possible configurations of the system is impractical (in most realistic applications $N \to \infty$), approximation schemes have been introduced which average exactly over the fluctuations confined to a small number of sites in the system. Over the years, this effort has led to a great number of approximate treatments of disorder within both non-self-consistent and self-consistent formalisms. Self-consistent theories fall in the category of mean-field theories, exemplified by the Weiss molecular theory of magnetism, and generally lead to results that provide a more accurate representation of physical properties.

A widely used method is the single-site coherent-potential approximation[1] (CPA), in which the effects of disorder are described by considering a single site embedded in an effective medium. The medium is determined in a self-consistent manner through the condition that the scattering of an electron (or wave) off the potential represented by the site embedded in this medium vanishes when averaged over its possible type α. While the CPA has generally proved to be the most satisfactory single-site approach to the study of disorder, its principle limitation is that it yields a self-energy that is site diagonal and hence $\mathbf{k}$ independent. In other words, nonlocal correlations in the disorder fluctuations are completely neglected. In particular, this means that the method is unable to take account of short-range-order (SRO) effects in a self-consistent manner. SRO is, for example, always present in the disordered phase of an alloy and can strongly influence physical properties and phase evolution.

The need to improve upon the CPA has motivated the development of a variety of cluster theories (see Ref. 2 for an extensive review). One of the better-known attempts is the molecular coherent-potential approximation[3–5] (MCPA), the properties of which are well understood. All one needs to do is replace the concept of a single site with that of a cluster whose periodic repetition generates the lattice to obtain the formal description of this approximation. Like the CPA, the MCPA is analytic and leads to a medium that is described by a cluster diagonal self-energy (as the single-site CPA leads to a site-diagonal one). However, such a generalization of the CPA violates one of the formal properties that must be satisfied by any self-consistent cluster theory[2] in that it leads to a medium which breaks the translational invariance of the underlying lattice. Although the MCPA accounts exactly for the statistical fluctuations within a cluster of sites, giving correctly such properties as densities of states associated with distinct cluster configurations,[2] the lack of translational invariance is a great drawback for the formal validity and practical viability of the theory. The edges of the reduced Brillouin zone (BZ) associated with a cluster superstructure can lead to spurious and hence unphysical scattering effects on wave propagation. Thus, for example, the study of electronic transport or phonons loses much of its formal integrity as the effects of this scattering cannot be easily corrected.[2]

The need to provide a description of SRO within a method that preserves the translational invariance of the underlying lattice has been keenly felt almost since the introduction of the CPA. In spite of great expenditure in formal and computational effort, only recently has a viable solution been proposed, namely, the nonlocal coherent-potential approximation (NLCPA) introduced by Jarrell and Krishnamurthy in Ref. 6. The method originates from the dynamical cluster approximation[7,8] (DCA) developed for describing nonlocal dynamical correlations in correlated electron systems. The NLCPA was subsequently developed within the framework of multiple-scattering theory [Korringa-Kohn-Rostoker (KKR)–NLCPA (Refs. 9–11)], and was recently combined with density-functional theory in Ref. 12, enabling

first-principles total-energy calculations to be carried out for realistic systems.

In contrast to the MCPA, the NLCPA handles correlations in the disorder fluctuations in reciprocal space. This is achieved by first dividing the lattice into *sublattices*, which in reciprocal space is equivalent to dividing the BZ into tiles. Therefore the full BZ of the underlying lattice is always considered as opposed to the smaller supercell BZ involved in the MCPA. Each sublattice is assumed to have its own self-energy, which is approximated as a constant in the reciprocal-space tile occupied by that sublattice. In other words, correlations in the disorder fluctuations between sites on the same sublattice are neglected. However correlations between sites on different sublattices remain. The medium is determined by mapping to a self-consistently embedded cluster with periodic Born–von Kármán boundary conditions imposed.

However, while many NLCPA calculations have appeared in the literature, until recently[13] the properties of the NLCPA had not been thoroughly investigated for the simplest case of a one-dimensional (1D) tight-binding model. This is the most difficult test case for a cluster theory since fluctuations are most significant in one dimension, and many previous attempts at cluster theories were found to be nonvalid only when tested for such a model.[2] Indeed, such an investigation was recently carried out for the NLCPA in Ref. 13, where some shortcomings of the theory were discovered. First, it was found that (for cluster sizes N_c larger than one site) the density of states (DOS) contains spurious features which cannot be identified in the DOS obtained by exact methods[14] or real-space cluster approximations such as the MCPA or embedded-cluster method[15] (ECM). These spurious features are particularly apparent for small values of N_c but systematically disappear as N_c increases. Second, it is known that for a given real-space cluster, the corresponding choice of "cluster momenta" (see Sec. II) is not unique.[8] By using a different choice of cluster momenta, a different set of results (also containing spurious features) was obtained in Ref. 13. Hence the NLCPA appears to be a nonunique theory. However, it was also found that the differences between these two sets of results systematically disappear as N_c increases. In fact, at some "critical"[16] cluster size N_{cr}, the differences become negligible,[17] at which point all spurious features in the DOS also disappear. A third (and related) unsatisfactory property of the NLCPA is that it yields a spectral function with jumps (discontinuities) resulting from approximating the self-energy as a step function in reciprocal space.[18]

In summary, the current formulation of the NLCPA (and DCA) may only be considered a unique and systematic correction to the CPA above a specific starting cluster size N_{cr}. Although the above issues can be avoided by using a cluster size larger than N_{cr}, this is not always computationally viable. More importantly, a valid cluster generalization of the CPA should always yield unique results for any given cluster size N_c, and should give systematic improvements as the cluster size increases from 1 to ∞. In this paper we introduce a reformulation of the NLCPA which satisfies these requirements and eliminates all the problems outlined above. In fact, it is shown that the previous formalism is a specific limiting case of the reformulation.

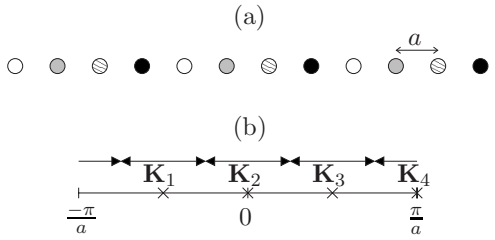

FIG. 1. (a) Division of a 1D lattice into $N_c=4$ sublattices. Each sublattice is represented by a different fill pattern and has a lattice constant $4a$. We may form a cluster of $N_c=4$ sites by taking a site from each sublattice. (b) Reciprocal-sublattice vectors $\mathbf{K}_n$ given by multiples of $2\pi/4a$. Each sublattice Brillouin zone (BZ) occupies a region of $\mathbf{k}$ space $N_c=4$ times smaller than the original lattice BZ. However, $N_c=4$ of these "tiles" (represented by double-headed arrows) together comprise the original lattice BZ.

The outline of this paper is as follows: First we briefly summarize the conventional NLCPA formalism in the context of a tight-binding Hamiltonian. We then describe the reformulation, detail the replacement algorithm, and show how to calculate properties. Finally, we show detailed results of the theory for the 1D tight-binding model, in particular the convergence properties of the DOS, self-energy, and spectral function.

II. FORMALISM

A. Conventional nonlocal coherent-potential approximation

Following Refs. 6 and 8, we provide a brief review of the conventional NLCPA here. In a basis labeled by the sites of the direct lattice, we will consider a tight-binding Hamiltonian with matrix elements

$$H^{ij} = \epsilon^i \delta_{ij} + W^{ij}(1 - \delta_{ij}), \tag{1}$$

where ϵ^i is the on-site energy at site i and W^{ij} is the parameter describing the hopping between site i and site j. Denoting a specific configuration of $\{\epsilon^i\}$ as γ and the corresponding Green's function for that configuration by G_γ, the exact average over all configurations may be written in the form

$$\langle G_\gamma^{ij} \rangle = G_0^{ij} + \sum_{k,l} G_0^{ik} \Sigma^{kl} \langle G_\gamma^{lj} \rangle, \tag{2}$$

where G_0^{ij} is the free-particle Green's function and Σ^{ij} is the exact self-energy. Equation (2) may be equivalently expressed in reciprocal space as

$$\langle G(\mathbf{k}) \rangle = G_0(\mathbf{k}) + G_0(\mathbf{k}) \Sigma(\mathbf{k}) \langle G(\mathbf{k}) \rangle. \tag{3}$$

Let us begin the discussion of the NLCPA by conceptualizing a real-space lattice with lattice constant a as a set of N_c sublattices. In reciprocal space this is equivalent to dividing the BZ of the lattice into N_c tiles, each centered at a reciprocal-sublattice vector $\mathbf{K}_n$, with $n=1,\ldots,N_c$. The lattice momenta $\mathbf{k}$ within a given tile n correspond to differences between sites on sublattice n with lattice constant $N_c a$ only. An illustrative example for a simple 1D lattice is given in Fig. 1. It is important to realize that at this stage no approximations have been made; the original lattice problem has

simply been reformulated in terms of N_c sublattices.

Next, let us consider an isolated cluster of N_c sites $\{I\}$ with periodic Born–von Kármán boundary conditions imposed. This can be visualized as each end mapping back to the other end along each axis; so, for example, in one dimension it is simply a ring of N_c sites. Clearly, the BZ of such a system contains N_c evenly spaced points in reciprocal space, referred to as the set of cluster momenta $\{\mathbf{K}_n\}$. The usual lattice Fourier transform becomes

$$\frac{1}{N_c}\sum_{\mathbf{K}_n} e^{i\mathbf{K}_n\mathbf{R}_{IJ}} = \delta_{IJ}, \tag{4}$$

where $\mathbf{R}_{IJ}$ is the vector distance between the centers of sites I and J. Averaged cluster quantities are translationally invariant and can be related in real and reciprocal spaces through Eq. (4). For example, we have the expressions

$$\Sigma^{IJ} = \frac{1}{N_c}\sum_{\mathbf{K}_n} \Sigma(\mathbf{K}_n) e^{i\mathbf{K}_n(\mathbf{R}_I-\mathbf{R}_J)} \tag{5}$$

and

$$\Sigma(\mathbf{K}_n) = \sum_J \Sigma^{IJ} e^{-i\mathbf{K}_n(\mathbf{R}_I-\mathbf{R}_J)} \tag{6}$$

for the cluster self-energy.

The cluster momenta and reciprocal-sublattice vectors have the same periodicity and we can choose these sets $\{\mathbf{K}_n\}$ to be equivalent. However in order to couple the cluster to the lattice while preserving translational invariance, two approximations are needed. The first is to approximate the exact lattice self-energy (for a disordered system) $\Sigma(\mathbf{k})$ as a step function passing through the values obtained from the cluster, i.e.,

$$\Sigma(\mathbf{k}) = \Sigma(\mathbf{K}_n) \tag{7}$$

for $\mathbf{k}$ lying within the nth reciprocal-space tile. In real space, this means that correlations between sites on the same sublattice are neglected and only correlations between sites on different sublattices remain. Thus the range of correlation included is restricted by the number of sublattices considered, or equivalently the size of the cluster.

The second approximation (which is an approximation even for a pure ordered system) is to set the phase factors $e^{i\mathbf{k}\cdot\mathbf{R}_{IJ}}$ to unity in the lattice Fourier transform. This means that the lattice Green's function in reciprocal space may be represented by the set of values

$$\bar{G}(\mathbf{K}_n) = \frac{N_c}{\Omega_{\mathrm{BZ}}}\int_{\Omega_{\mathbf{K}_n}} d\mathbf{k}[E - W(\mathbf{k}) - \Sigma(\mathbf{K}_n)]^{-1}, \tag{8}$$

since we are now free to sum over the dispersion within each tile. These values are straightforward to calculate since $\Sigma(\mathbf{K}_n)$ is constant (coarse grained) within each tile $\Omega_{\mathbf{K}_n}$. This approximation has been proven[6] to be causal (analytic), and physically it removes information about the relative location of the cluster sites to the lattice. Therefore each cluster site is coupled to the effective medium in exactly the same way irrespective of its location within the cluster. Using Eq. (4), the real-space Green's function at the cluster sites becomes

$$\bar{G}^{IJ} = \frac{1}{\Omega_{\mathrm{BZ}}}\sum_{\mathbf{K}_n}\int_{\Omega_{\mathbf{K}_n}} d\mathbf{k}[E - W(\mathbf{k}) - \Sigma(\mathbf{K}_n)]^{-1} e^{i\mathbf{K}_n(\mathbf{R}_I-\mathbf{R}_J)}. \tag{9}$$

Finally, while the above describes how correlations in the fluctuations are handled in $\mathbf{k}$ space, the fluctuations themselves must be defined in real space. To do that, we must first define the reciprocal-space cavity Green's function $\mathcal{G}(\mathbf{K}_n)$ via the Dyson equation

$$\bar{G}(\mathbf{K}_n) = \mathcal{G}(\mathbf{K}_n) + \mathcal{G}(\mathbf{K}_n)\Sigma(\mathbf{K}_n)\bar{G}(\mathbf{K}_n), \tag{10}$$

which is introduced to avoid overcounting self-energy contributions from the cluster. Equation (10) can also be expressed in real space by applying Fourier transform equation (4) to yield the expression

$$\bar{G}^{IJ} = \mathcal{G}^{IJ} + \sum_{K,L} \mathcal{G}^{IK}\Sigma^{KL}\bar{G}^{LJ}. \tag{11}$$

While $\mathcal{G}^{IJ}$ is independent of the chemical occupation of the cluster itself, note that it differs from the analogous quantity introduced in the ECM and MCPA since it does not have a real-space expansion. Nevertheless, an impurity cluster Green's function may be defined by replacing the cluster self-energy in Eq. (11) with a particular configuration of site energies $\{\epsilon_\alpha^I\}$, i.e.,

$$G_\gamma^{IJ} = \mathcal{G}^{IJ} + \sum_K \mathcal{G}^{IK}\epsilon_\alpha^K G_\gamma^{KJ}. \tag{12}$$

The NLCPA imposes the self-consistency condition

$$\sum_\gamma P_\gamma G_\gamma^{IJ} = \bar{G}^{IJ}, \tag{13}$$

where P_γ is the probability of configuration γ occurring, appropriately weighted to include SRO if desired. The effective medium is therefore determined from a self-consistent solution of Eqs. (9) and (13). See Ref. 6 for details of the algorithm. The formalism reduces to the CPA for $N_c=1$ and becomes exact as $N_c\to\infty$.

B. Reformulation

As described above, the conventional NLCPA imposes periodic Born–von Kármán boundary conditions on the cluster with the relationship between the cluster sites and cluster momenta defined through Eq. (4).[6] Since Eq. (4) is simply a discretized version of the usual lattice Fourier transform as a result of having only N_c sites in the system, it is important to observe that the lattice constant remains unchanged and hence the cluster BZ has the same dimensions as the lattice BZ. Next, observe that for a given real-space cluster there are in fact an infinite number of solutions to Eq. (4). Conventionally, the set of cluster momenta which includes the origin $\mathbf{K}_n=(0,0,0)$ for some n in reciprocal space has been chosen, a convention adopted in all later implementations. However by fixing the BZ origin at, say, (0,0,0) and including some arbitrary phase ϕ such that

$$\frac{1}{N_c}\sum_n e^{i(\mathbf{K}_n\cdot\mathbf{R}_{IJ}-\phi)} = \delta_{IJ}, \tag{14}$$

we see that a continuous distribution of solutions are possible. By writing ϕ in the form $\phi=\Sigma_d\phi_d$, where $d=x$, y, or z, the phase can be varied in each spatial direction independently. For a 1D or two-dimensional (2D) square or a three-dimensional (3D) cubic system, the components of the possible cluster momenta values are then given by

$$K_{nd} = \frac{\phi_d}{N_c^{1/D}a} - \frac{2\pi n}{N_c^{1/D}a} \quad \text{for} \quad n = 1, \ldots, N_c, \tag{15}$$

where a is the lattice constant, D is the number of dimensions, and $0\leq\phi_d\leq 2\pi$ (with a periodicity of 2π) for each $d=x,y,z$. Similar relations can be found for any given lattice.

Notation. Since we can select phases in each direction d independently, let us define a set of phases $\{\phi_d\}$ as a set of D values (where D is the dimensionality) containing one value in each direction d. We can then write $\mathbf{K}_n=\mathbf{K}_n\{\phi_d\}$ in order to label the cluster momenta values by the choice of set $\{\phi_d\}$, and Eq. (14) becomes

$$\frac{1}{N_c}\sum_n e^{i\mathbf{K}_n\{\phi_d\}\mathbf{R}_{IJ}} = \delta_{IJ}. \tag{16}$$

For clarity during the following derivation and discussion, we will assume three dimensions so that $\mathbf{K}_n=\mathbf{K}_n(\phi_x,\phi_y,\phi_z)$.

It is clear that ϕ_d has the effect of shifting the positions of the (evenly spaced) cluster momenta in direction d within the BZ. Of course, for an isolated cluster with Born–von Kármán boundary conditions, it is possible to similarly shift the BZ origin and hence phase differences are irrelevant. However, the situation is different in the NLCPA when we couple the cluster to the lattice in reciprocal space. First let us fix the cluster BZ origin *relative* to the lattice BZ origin, and label this difference as ΔO_{BZ} (e.g., zero). The next step is to divide the lattice BZ into tiles centered at the cluster momenta, and approximate the (unknown) lattice self-energy $\Sigma(\mathbf{k})$ as a step function via

$$\Sigma(\mathbf{k}) = \Sigma[\mathbf{K}_n(\phi_x,\phi_y,\phi_z)] \tag{17}$$

within each tile n, meaning only correlations between sites on different sublattices are included. Since ΔO_{BZ} is fixed, the values of the cluster momenta are fixed relative to the lattice momenta $\{\mathbf{k}\}$. Significantly, it follows that changing any of the phases $\{\phi_x,\phi_y,\phi_z\}$ will yield a *different* step function. In turn, the configurationally averaged Green's function for a cluster of N_c sites in real space now depends on the choice of phases. Each $\bar{G}(\phi_x,\phi_y,\phi_z)$ describes a different NLCPA medium and hence calculated physical observables also vary with respect to the choice of $\{\phi_x,\phi_y,\phi_z\}$. An example of the BZ tiling as a function of ϕ_x for a 1D lattice is illustrated in Fig. 2.

In summary, the approximation made via Eq. (17) introduces a dependence on phase (or equivalently a dependence on choice of cluster momenta) into the system. This dependence must be eliminated in order to obtain a unique theory,

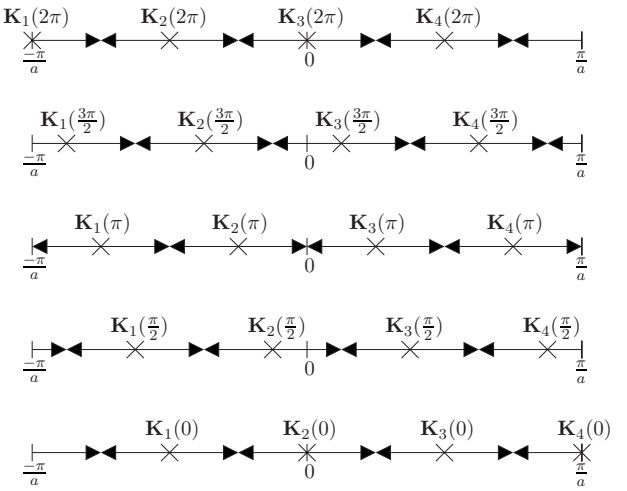

FIG. 2. BZ tiling for a selection of values of ϕ_x for a 1D lattice with $N_c=4$. The selection is taken from the continuous distribution of available values $0\leq\phi_x\leq 2\pi$. The $\mathbf{K}_n(\phi_x)$ points are marked by crosses, and the corresponding tiles by double-headed arrows. Observe the symmetry about the central value in the distribution $\phi_x=\pi$. For example, the $\mathbf{K}_n(\phi_x)$ points and corresponding tiling are equivalent for the extreme values $\phi_x=0$ and $\phi_x=2\pi$.

i.e., an averaged Green's function that is unique for a given cluster size. To achieve this, it is clear that in addition to averaging over all cluster configurations at each iteration in the algorithm via the sum

$$\bar{G}^{IJ}(\phi_x,\phi_y,\phi_z) = \sum_\gamma P_\gamma G_\gamma^{IJ}(\phi_x,\phi_y,\phi_z) \tag{18}$$

for a given set of $\{\phi_x,\phi_y,\phi_z\}$, we must also average over all possible phases via the expression

$$\bar{G}^{IJ} = \frac{1}{(2\pi)^D}\int_0^{2\pi}\int_0^{2\pi}\int_0^{2\pi} d\phi_x d\phi_y d\phi_z \bar{G}^{IJ}(\phi_x,\phi_y,\phi_z). \tag{19}$$

This yields an averaged Green's function that is unique for a given cluster size N_c, and so calculated physical observables no longer depend on an individual choice of phases. If we discretize the continuous distribution in Eq. (19) by including only a finite number of phases, we can minimize the error in the moments by including an appropriate weighting distribution.[19]

There are two important points to appreciate about Eq. (19). First, it should be noted that in the original formulation of the NLCPA (Ref. 6) [and DCA (Ref. 8)], all choices of phase other than $(\phi_x,\phi_y,\phi_z)=(0,0,0)$ and $(\phi_x,\phi_y,\phi_z)=(\pi,\pi,\pi)$ were ruled out since the corresponding reciprocal-space tilings do not preserve the point-group symmetry of the underlying lattice. This can be seen from Fig. 2 in one dimension where certain equivalent lattice momenta $\mathbf{k}$ (i.e., certain pairs of values symmetric about the origin) are mapped to nonequivalent tiles for all choices other than $\phi_x=0$ (or 2π) and $\phi_x=\pi$. However, in the reformulation presented here, point-group symmetry is naturally restored when averaging over all possible choices of phases via Eq.

(19). Moreover, Eq. (19) preserves the crucial requirement of causality since it is a sum of functions which are themselves causal (analytic).

While averaging the Green's function over all phases in real space via Eq. (19) is intuitively clear, we need to express Eq. (19) in **k** space in order to proceed further and develop an algorithm to determine the new medium. We will see that the resulting expression is equivalent to averaging over all possible choices of cluster momenta.

From the solutions given by Eq. (15), we obtain the relations

$$d\phi_x = (N_c^{1/D}a)dK_{nx},$$

$$d\phi_y = (N_c^{1/D}a)dK_{ny},$$

$$d\phi_z = (N_c^{1/D}a)dK_{nz}, \tag{20}$$

which we can use to change the variables in Eq. (19). Changing variables together with substituting the relation

$$\bar{G}^{IJ}(\phi_x,\phi_y,\phi_z) = \frac{1}{N_c}\sum_n \bar{G}[\mathbf{K}_n(\phi_x,\phi_y,\phi_z)]e^{i[\mathbf{K}_n(\phi_x,\phi_y,\phi_z)]\cdot\mathbf{R}_{IJ}} \tag{21}$$

yields the expression

$$\bar{G}^{IJ} = \left(\frac{a}{2\pi}\right)^D \sum_n \int d\mathbf{K}_n \bar{G}[\mathbf{K}_n(\phi_x,\phi_y,\phi_z)]e^{i[\mathbf{K}_n(\phi_x,\phi_y,\phi_z)]\cdot\mathbf{R}_{IJ}}, \tag{22}$$

where the notation implies that

$$\int d\mathbf{K}_n = \int_{K_{nx}(0)}^{K_{nx}(2\pi)} \int_{K_{ny}(0)}^{K_{ny}(2\pi)} \int_{K_{nz}(0)}^{K_{nz}(2\pi)} dK_{nx}(\phi_x)dK_{ny}(\phi_y)dK_{nz}(\phi_z). \tag{23}$$

Here

$$\bar{G}[\mathbf{K}_n(\phi_x,\phi_y,\phi_z)] = \int_{\Omega_{\mathbf{K}_n(\phi_x,\phi_y,\phi_z)}} d\mathbf{k}\{E - W(\mathbf{k}) - \Sigma[\mathbf{K}_n(\phi_x,\phi_y,\phi_z)]\}^{-1}, \tag{24}$$

where $\Omega_{\mathbf{K}_n(\phi_x,\phi_y,\phi_z)}$ is the volume of the reciprocal-space tile associated with the cluster momentum point $\mathbf{K}_n(\phi_x,\phi_y,\phi_z)$. By substituting Eq. (24) into Eq. (22) and then reversing the order of the integrals, we arrive at the result

$$\bar{G}^{IJ} = \frac{1}{\Omega_{\mathrm{BZ}}}\sum_n \int_{\Omega_{\mathbf{K}_n(\phi_x,\phi_y,\phi_z)}} d\mathbf{k} e^{i[\mathbf{K}_n(\phi_x,\phi_y,\phi_z)]\cdot\mathbf{R}_{IJ}} \times \int d\mathbf{K}_n\{E - W(\mathbf{k}) - \Sigma[\mathbf{K}_n(\phi_x,\phi_y,\phi_z)]\}^{-1}. \tag{25}$$

The volume integration over **k** in the first integral simply equates to an integral over the first BZ for any choice of phases. Therefore the **k**-space Green's function can be defined as a sum over all possible choices of cluster momenta in the form

$$\bar{G}(\mathbf{k}) = \int d\mathbf{K}_n\{E - W(\mathbf{k}) - \Sigma[\mathbf{K}_n(\phi_x,\phi_y,\phi_z)]\}^{-1}, \tag{26}$$

where $d\mathbf{K}_n$ has been defined through Eq. (23) and the sum includes the appropriate set of $\Sigma[\mathbf{K}_n(\phi_x,\phi_y,\phi_z)]$ associated with the point **k**.

This completes the formal relations needed to derive an algorithm. The idea is to self-consistently determine the medium self-energy at each point $\mathbf{K}_n\{\phi_d\}$, where $n=1,\ldots,N_c$ and each ϕ_d takes a selection of values in the range $0 \le \phi_d \le 2\pi$ for $d=x,y,z$. Let us denote the number of sets of phases $\{\phi_d\}$ included by N_p. It is clear that as we increase N_p, we will get a more accurate description of the medium self-energy for a given cluster size N_c. While the reformulation reduces to the conventional formalism for $N_p=1$, in contrast the self-energy will no longer be a simple step function for $N_p>1$. In fact if we include a sufficient number of phases such that the number of $\mathbf{K}_n\{\phi_d\}$ points is equivalent to the number of **k** points in the BZ, then we can calculate the self-energy correctly (**k** point by **k** point) for a given cluster size.

C. Replacement algorithm

(1) Begin with a guess for the (fully **k**-dependent) medium self-energy $\Sigma(\mathbf{k})$, e.g., zero.

(2) For each n (where $n=1,\ldots,N_c$), sample $\Sigma(\mathbf{k})$ at a selection of N_p sets of phases $\{\phi_d\}$, yielding the values $\{\Sigma(\mathbf{K}_n\{\phi_d\})\}$.

(3) Calculate the set of "coarse-grained" Green's functions,

$$\bar{G}(\mathbf{K}_n\{\phi_d\}) = \int_{\Omega_{\mathbf{K}_n\{\phi_d\}}} d\mathbf{k}[E - W(\mathbf{k}) - \Sigma(\mathbf{K}_n\{\phi_d\})]^{-1},$$

for each n and each set of phases $\{\phi_d\}$.

(4) Calculate the **k**-space cavity Green's function at the set of sample points via the equation

$$\mathcal{G}(\mathbf{K}_n\{\phi_d\}) = [\bar{G}(\mathbf{K}_n\{\phi_d\})^{-1} + \Sigma(\mathbf{K}_n\{\phi_d\})]^{-1},$$

and convert to real space using the relation

$$\mathcal{G}^{IJ}\{\phi_d\} = \frac{1}{N_c}\sum_n \mathcal{G}(\mathbf{K}_n\{\phi_d\})e^{i\mathbf{K}_n\{\phi_d\}\cdot\mathbf{R}_{IJ}}.$$

(5) Calculate the impurity Green's function

$$\underline{G}_\gamma\{\phi_d\} = \underline{\mathcal{G}}\{\phi_d\} + \underline{\mathcal{G}}\{\phi_d\}\underline{V}_\gamma\underline{G}_\gamma\{\phi_d\}$$

for each set $\{\phi_d\}$, where V_γ is an impurity cluster configuration. Here an underscore denotes a matrix in the space of the cluster sites.

(6) *Sum over all configurations;* i.e., calculate the configurationally averaged Green's function by summing over all impurity cluster configurations,

$$\bar{G}^{IJ}\{\phi_d\} = \sum_\gamma P_\gamma G_\gamma^{IJ}\{\phi_d\}$$

for each set $\{\phi_d\}$, where P_γ is the probability of configuration γ occurring.

(7) Calculate the new (phase-dependent) self-energy $\Sigma_\phi^{IJ}\{\phi_d\}$ via the equation

$$\underline{\Sigma}_\phi\{\phi_d\} = \underline{\mathcal{G}}\{\phi_d\}^{-1} - \underline{\bar{G}}\{\phi_d\}^{-1},$$

and convert to $\mathbf{k}$ space through the relation

$$\Sigma_\phi(\mathbf{K}_n\{\phi_d\}) = \sum_J \Sigma_\phi^{IJ}\{\phi_d\} e^{-i\mathbf{K}_n\{\phi_d\}\cdot\mathbf{R}_{IJ}}$$

for each n and each set $\{\phi_d\}$.

(8) *Sum over all phases;* i.e., calculate the (fully $\mathbf{k}$-dependent) medium Green's function

$$\bar{G}(\mathbf{k}) = \int d\mathbf{K}_n [E - W(\mathbf{k}) - \Sigma_\phi(\mathbf{K}_n\{\phi_d\})]^{-1},$$

where

$$\int d\mathbf{K}_n = \int_{K_{nx}(0)}^{K_{nx}(2\pi)} \int_{K_{ny}(0)}^{K_{ny}(2\pi)} \int_{K_{nz}(0)}^{K_{nz}(2\pi)} dK_{nx}(\phi_x) dK_{ny}(\phi_y) dK_{nz}(\phi_z)$$

in three dimensions, and the sum includes the appropriate set of $\Sigma_\phi(\mathbf{K}_n\{\phi_d\})$ associated with the point $\mathbf{k}$.

(9) Calculate the new (fully $\mathbf{k}$-dependent) medium self-energy $\Sigma^{\text{new}}(\mathbf{k})$ via the Dyson equation,

$$\Sigma^{\text{new}}(\mathbf{k}) = E - W(\mathbf{k}) - \bar{G}(\mathbf{k})^{-1}.$$

Due to the averaging in step 8, this is now uniquely defined at each $\mathbf{k}$ point.

(10) Compare $\Sigma^{\text{new}}(\mathbf{k})$ with the old $\Sigma(\mathbf{k})$ in step 1. If they are not equivalent within some prescribed tolerance, then repeat the algorithm from step 2 until convergence is achieved. The equivalent algorithm for implementation in first-principles KKR codes is given in the Appendix.

D. Notes on the algorithm

Convergence condition. While the algorithm determines a fully $\mathbf{k}$-dependent medium self-energy, in practice it is only necessary to ensure convergence at the sample points.

Short-range order. Short-range order can be self-consistently included by incorporating an appropriate non-random probability distribution $\{P_\gamma\}$ when averaging over the configurations in step 6 of the algorithm. The distribution should be chosen to preserve the symmetries of the underlying lattice.

Computational time. While the computational cost scales as N_p, this is partially offset since the algorithm converges much more quickly for $N_p > 1$. This is because the solution becomes more stable as N_p increases since we are getting closer to the correct effective medium. For example, the total number of iterations required is reduced by more than half when increasing $N_p = 1$ to $N_p = 2$ for the 1D calculations presented later in this paper. Computational time can be reduced further by utilizing symmetry when selecting the phases (see below). Also, computational time can be saved by using a fast Fourier transform (FFT) algorithm to implement the discrete Fourier transforms in steps 4 and 7.

Choice of phases. While the cluster momenta corresponding to a given set of phases $\{\phi_d\}$ are always evenly spaced, the distribution of the phases themselves is arbitrary. If computational time is not an issue, one can simply choose the phases to be evenly spaced in each direction (in which case the integration in step 8 of the algorithm conveniently reduces to a simple average) and include a sufficient number to ensure convergence. Otherwise, the spacings should be chosen to minimize the error in the moments. This could also involve the introduction of a weighting distribution $\{\gamma_{\{\phi_d\}}(\mathbf{k})\}$ (with elements tending to unity as $N_p \to \infty$) which can be included when averaging over all phases in step 8 of the algorithm. This would optimize the convergence of the medium (and hence bulk properties) with respect to N_p and hence minimize the value of N_p required to ensure convergence. The optimum distribution of phases and weighting function for use in realistic NLCPA calculations is currently being investigated.

Point-group symmetry. Only the sets $(\phi_x, \phi_y, \phi_z) = (0,0,0)$ and $(\phi_x, \phi_y, \phi_z) = (\pi, \pi, \pi)$ individually preserve the point-group symmetry of the lattice if only one set is included in the calculation (i.e., $N_p = 1$). However, for $N_p > 1$, point-group symmetry will be restored when averaging over all N_p sets $\{\phi_d\}$ provided one avoids choosing sets that are not symmetric to each other about $(\phi_x, \phi_y, \phi_z) = (\pi, \pi, \pi)$. This problem can be avoided (and computational time can be saved) by choosing sets $\{\phi_d\}$ only from the irreducible part of the tile centered at $\mathbf{K}_n(\pi, \pi, \pi)$ for $n = 1, \ldots, N_c$, and then utilizing point-group symmetry in the calculation.

E. Calculating properties

Once the algorithm has converged, the averaged density of states for the system is given by

$$n(E) = -\frac{1}{\pi} \text{Im } \bar{G}^{II}, \tag{27}$$

where $\bar{G}^{II}$ is the site-diagonal part of the phase-independent configurationally averaged Green's function, and any cluster site I may be chosen because of translational invariance. $\bar{G}^{II}$ is most straightforwardly obtained from the BZ integral,

$$\bar{G}^{II} = \frac{1}{\Omega_{\text{BZ}}} \int_{\Omega_{\text{BZ}}} d\mathbf{k} \bar{G}(\mathbf{k}), \tag{28}$$

where $\bar{G}(\mathbf{k})$ is defined by Eq. (26) and is calculated at step 8 of the algorithm above. Similarly, the Bloch spectral function is obtained from $\bar{G}(\mathbf{k})$ via the expression

$$A^B(\mathbf{k}) = -\frac{1}{\pi} \text{Im } \bar{G}(\mathbf{k}) \tag{29}$$

for a given energy.

Since the reformulation is fully self-consistent, we can also obtain partially averaged (component) density of states. To do that, we must first calculate the (phase-dependent) impurity Green's function $\underline{G}_\gamma\{\phi_d\}$ for a given cluster configuration γ. This is defined by Eq. (18) and is calculated at step 5 of the algorithm. We must then sum over all phases in real space via the expression

$$G_\gamma^{IJ} = \frac{1}{(2\pi)^D}\int_0^{2\pi}\int_0^{2\pi}\int_0^{2\pi} d\phi_x d\phi_y d\phi_z G_\gamma^{IJ}(\phi_x,\phi_y,\phi_z). \tag{30}$$

(Note that if the phases have been chosen to be evenly spaced, then the above integration simply reduces to a simple average.) For a given cluster configuration γ, the partially averaged (cluster component) DOS measured on any site I is then given by the matrix element G_γ^{II}. Furthermore, single-site component DOS may be defined at a cluster site I by averaging G_γ^{II} over all configurations γ' which contain site I as the desired species α, i.e.,

$$G_\alpha^{II} = \sum_{\gamma'} P_{\gamma'} G_{\alpha,\gamma'}^{II}, \tag{31}$$

where the notation implies that site I is a site of species α, γ' is a configuration of the remaining sites in the cluster, and $P_{\gamma'}$ is the probability of that configuration occurring. Again, the $\{G_\alpha^{II}\}$ are independent of the choice of cluster site I because of translational invariance.

F. Comparison with the molecular coherent-potential approximation

The MCPA and NLCPA are two different, although complementary, approaches to treating disorder. The MCPA treats correlations in real space, whereas the NLCPA primarily handles correlations in reciprocal space. The differences between the analogous theories for strongly correlated systems, namely, the cellular dynamical mean-field theory[20] (DMFT) and DCA,[7,8] were thoroughly analyzed in Ref. 21. However, the differences between the MCPA and NLCPA are often misunderstood in the literature and the NLCPA is often incorrectly interpreted as a supercell-type calculation.[22–24] It is therefore worth discussing the main differences between the two theories here.

The MCPA divides the lattice into periodically repeating clusters, each with open boundary conditions. In other words, the self-energy is cluster diagonal and hence there are no self-energy terms linking sites in different clusters. Quantities are not translationally invariant *within* each cluster, and hence the corresponding medium has cluster (supercell) periodicity.

In contrast, the NLCPA divides the lattice into sublattices, and a compact cluster may be formed anywhere by taking a site from each sublattice. Phase factors containing information about the relative location of sites within the cluster to sites in the medium are neglected and hence each cluster site is topologically equivalent. By mapping to a cluster with periodic Born–von Kármán boundary conditions imposed (i.e., a ring in one dimension), the resulting medium has the single-site translational invariance of the underlying lattice. It is only the range of correlations included that is restricted by the number of sublattices considered (size of cluster) and so the self-energy Σ^{IJ} always has terms linking sites within the range $\mathbf{R}_I - \mathbf{R}_J$.

These two contrasting approaches to the treatment of correlations mean that there are marked differences in results obtained from the two theories.[13] Band edges and gaps are treated less accurately by the MCPA due to its supercell periodicity. On the other hand, the NLCPA neglects phase factors containing topological information within the cluster and hence yields less fine structure in the DOS than the MCPA. Indeed, the DOS measured on the central site in the MCPA converges to the exact result more quickly than the DOS obtained from the NLCPA, although the (reformulated) NLCPA shows convergence properties which can be considered very systematic with increasing cluster size.

III. RESULTS

In order to investigate the reformulation explicitly, results are presented for the 1D tight-binding model with diagonal disorder and nearest-neighbor hopping. This is the most difficult test case since fluctuations are most significant in one dimension. Furthermore, detailed structure is expected in the DOS which can be compared with the exact DOS obtainable by numerical means in one dimension.[14]

For N_c even, the set of cluster momenta in one dimension is given by

$$\{\mathbf{K}_n(\phi_x)\} = \frac{(2n - N_c)\pi - \phi_x}{N_c a}, \quad n = 1, \ldots, N_c \tag{32}$$

for a given ϕ_x, where ϕ_x can take a value in the range $0 \leq \phi_x < 2\pi$ (with a periodicity of 2π). When performing calculations with more than one phase included, we choose the values to be evenly spaced so that $\phi_x^m = (2\pi m)/N_p$, where N_p is the number of phases and $m = 1, \ldots, N_p$. We have also set the elements of the weighting distribution $\{\gamma_{\phi_x}(\mathbf{k})\}$ to unity for all values of N_p.

We have taken the site energies to be $\epsilon_A = +2.0$ and $\epsilon_B = -2.0$ with random probability (i.e., no short-range order), and the nearest-neighbor hopping parameter to be $W = 1.0$. This corresponds to the "split-band" regime, where the pure bands are just touching as previously investigated in Refs. 2 and 13. The pure bands together with the exact numerical result for a random $A_{50}B_{50}$ alloy (obtained using the negative eigenvalue theorem[14]) are shown in Figs. 3(a)–3(c). Figure 3(d) shows the CPA result for the same $A_{50}B_{50}$ alloy, with the smooth structure due to the neglect of nonlocal correlations being apparent. See Ref. 13 for a more detailed discussion of this model.

First, in order to demonstrate the nonuniqueness of the conventional formalism, a selection of DOS results obtained with a cluster size of $N_c = 2$ are shown in Fig. 4. As discussed

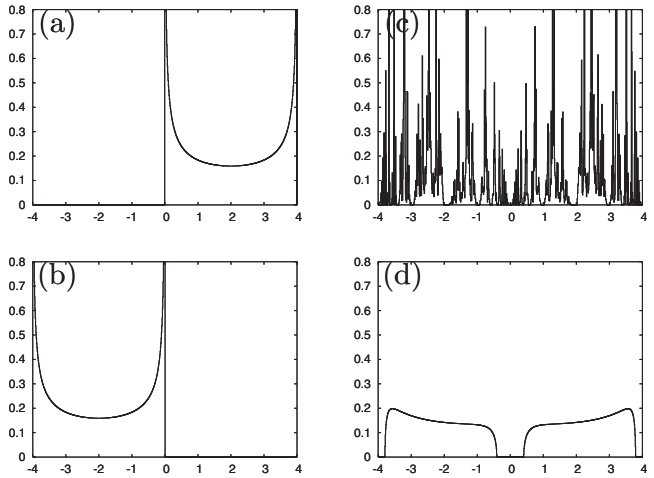

FIG. 3. (a) DOS (as a function of energy) for a pure material comprised of A sites, with $\epsilon_A=+2.0$. (b) DOS for a pure material comprising of B sites, with $\epsilon_B=-2.0$. (c) Exact DOS results for a random $A_{50}B_{50}$ alloy of the pure materials above. (d) DOS for the same $A_{50}B_{50}$ alloy obtained using the CPA.

previously,[13] the conventional $\phi_x=0$ choice contains spurious structure such as large troughs at $E=\pm 1.5$ not seen in the exact calculation in Fig. 3(c) or with calculations using real-space cluster methods such as the ECM or MCPA. As the value of ϕ_x is increased, the change in the structure of the DOS is apparent. Eventually at $\phi_x=\pi$ we obtain a DOS equivalent to the single-site CPA, where correlations are completely neglected. Such spurious features are accentuated further if short-range order is included by weighting the probabilities in the ensemble average.

In order to examine the extent to which the unique reformulation of the NLCPA bridges the gap between the CPA and exact result, Fig. 5 shows DOS results for the same $A_{50}B_{50}$ alloy obtained using the NLCPA for a selection of cluster sizes N_c (left to right) as a function of the number of phases included N_p (top to bottom). The $N_c=1$ result (CPA) is of course independent of N_p. The $N_p=1$ result shown here is obtained using the $\phi_x=0$ value conventionally used in the old formalism and contains spurious features as noted above. However, here we see that such features are removed as N_p is increased. In fact, for a given cluster size the correct DOS is formally obtained when $N_p\rightarrow\infty$. However in practice we see that far fewer phases are generally needed; e.g., for $N_c=2$ any changes are numerically insignificant above a "critical" value $N_p=8$. It is also apparent that the number of phases needed for convergence generally decreases as N_c increases. This is because the increased number of cluster momenta means the BZ is being more densely sampled to begin with. In fact, only one phase is required when $N_c\geq 12$ to obtain the correct DOS for the given cluster size for this 1D model (this is however not true for the spectral function; see below). As N_c is increased further beyond $N_c=12$ (not shown here), the DOS by definition eventually converges to the exact result in Fig. 3(c).

In order to gain some insight into the DOS results, Fig. 6 shows the imaginary part of the **k**-space self-energies calculated using the NLCPA at an example energy of $E=\pm 3.0$.

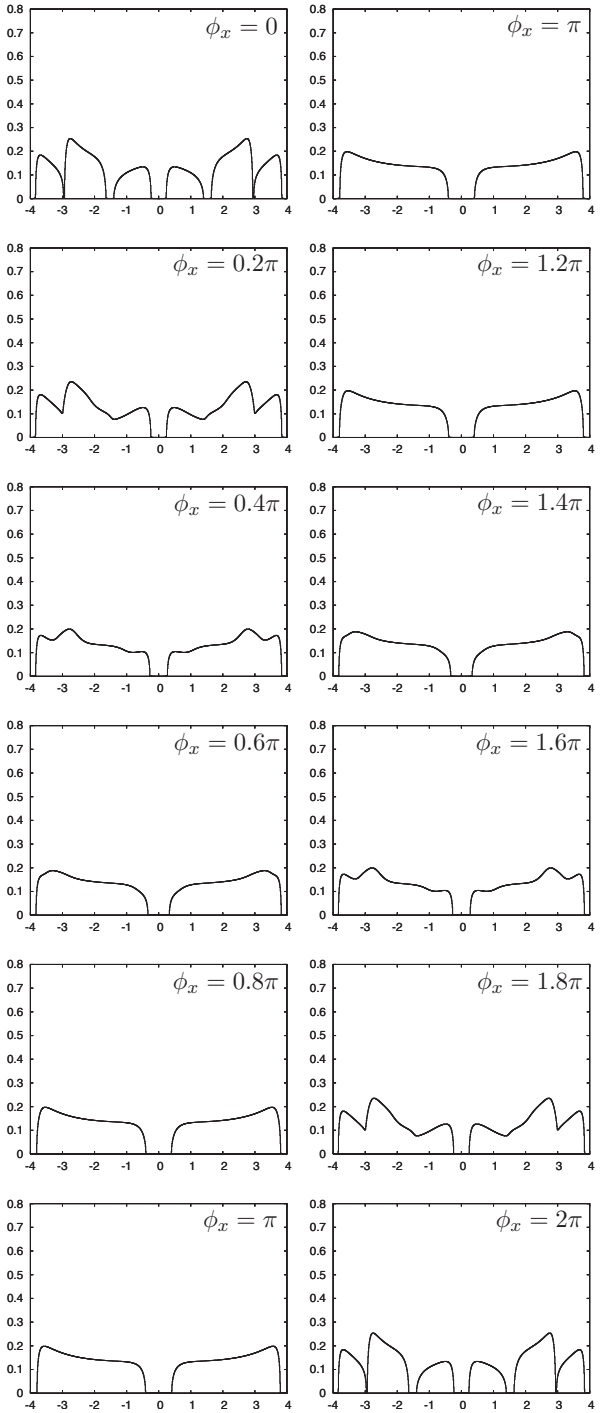

FIG. 4. Results for the configurationally averaged DOS per site as a function of energy obtained using the conventional NLCPA with cluster size $N_c=2$. A selection from the continuous distribution of available (nonunique) results is shown. Each calculation uses a different phase ϕ_x and the distribution is symmetric about the central value π with periodicity of 2π. However, only the $\phi_x=0$ (or 2π) and $\phi_x=\pi$ calculations individually preserve the point-group symmetry of the underlying lattice. Notice that the $\phi_x=\pi$ result is equivalent to the single-site CPA. This is because the self-energy is necessarily a constant in **k** space (owing to the symmetry of the cluster momenta about the BZ origin). Hence all nearest-neighbor correlation is removed; i.e., the cluster is in antiphase with the lattice.

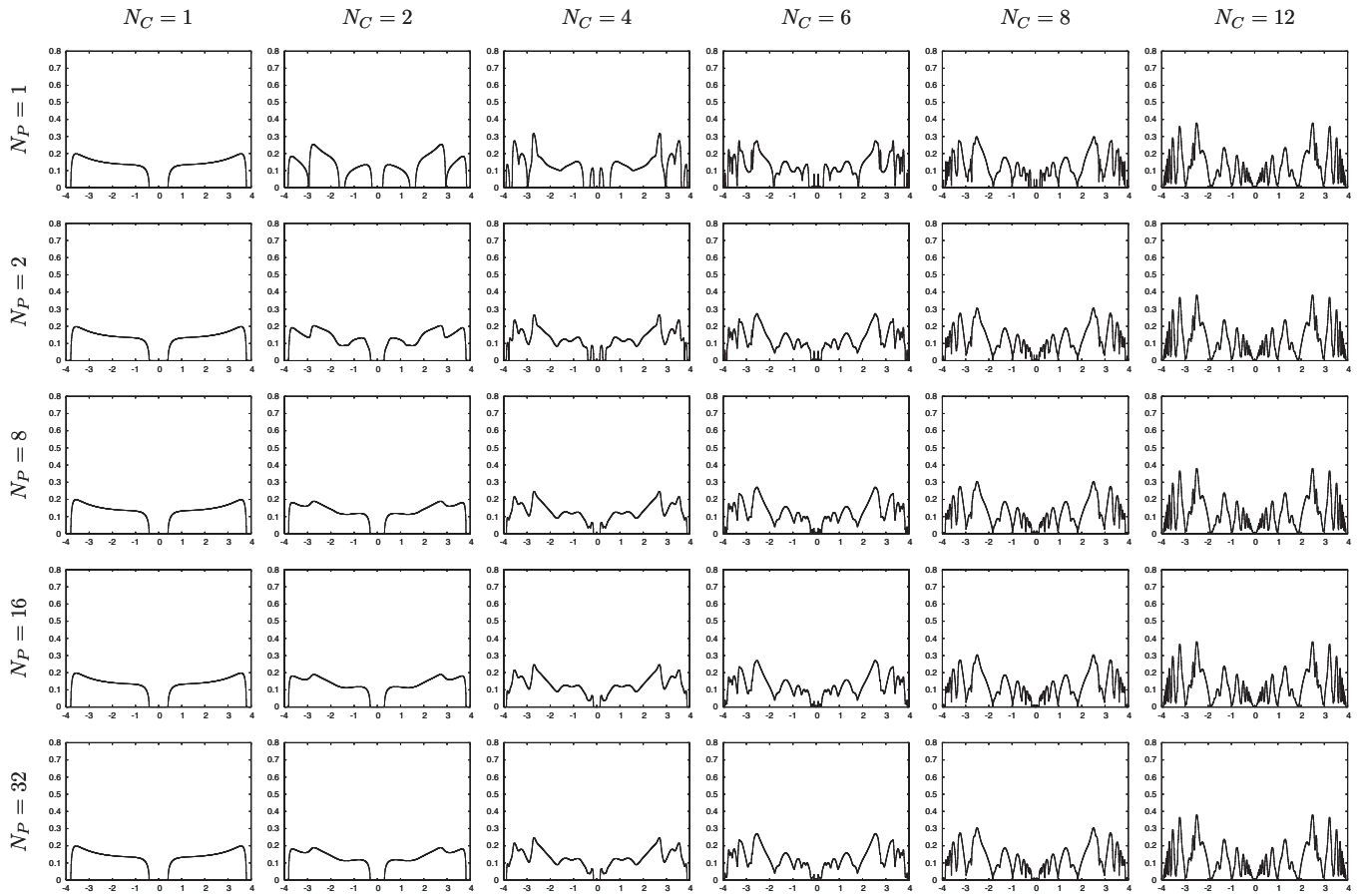

FIG. 5. Configurationally averaged DOS per site as a function of energy (in units of the bandwidth) obtained using the NLCPA as a function of cluster size N_c (left to right) and number of phases included N_p (top to bottom). The single phase result is for the conventional $\phi_x=0$ choice.

Again, results are shown for a selection of cluster sizes N_c as a function of the number N_p of phases included. First observe that the $N_c=1$ (CPA) result is a constant since the CPA self-energy is independent of both $\mathbf{k}$ and N_p. As N_c increases, we see that the self-energy for $N_p=1$ is the familiar step function of the old formalism with large discontinuities at the $\mathbf{k}$-space tile boundaries. This is particularly evident for $N_c=2$. As N_p is increased, it is apparent how we get closer and closer to the correct self-energy for the given cluster size N_c as the number of steps increases and the step function smoothens into a curve. Since we are now averaging over $N_p \times N_c$ $\mathbf{k}$-space tiles, formally the self-energy will only become completely smooth in the continuous limit $N_p \rightarrow \infty$.

Figure 7 shows the spectral functions corresponding to the self-energy graphs in Fig. 6 at the same example energy of $E= \pm 3.0$. First, observe that for $N_p=1$, the discontinuities in the spectral function can be large even for large cluster sizes where the self-energy has more initial steps. In a similar fashion to the self-energies in Fig. 6, while the number of discontinuities increases as N_p increases, the size of the discontinuities decreases and the convergence toward the correct spectral function for a given cluster size is clear. We also see that since the spectral function is a more sensitive quantity than the DOS, a higher value for N_p is generally required to obtain the correct spectral function here than that needed to obtain the correct DOS seen in Fig. 5. For example, more than one phase is still needed at $N_c=12$.

Finally, it should be pointed out that below the critical value for N_p, a different choice for the distribution of sets $\{\phi_d\}$ will yield different results. However, since calculations for simple 1D and 2D models are not computationally expensive, convergence with respect to N_p and hence unique results can be easily ensured. In principle, however, the spacing of the phases (together with an appropriate weighting distribution) should be chosen to minimize the error in the moments. This would optimize the convergence and hence minimize the critical value of N_p.

IV. CONCLUSIONS

A reformulation of the nonlocal coherent-potential approximation has been presented which yields a unique configurationally averaged Green's function for a given cluster size. It has been demonstrated that this reformulation is necessary in order to calculate physical quantities correctly within the NLCPA.

A key feature of the reformulation is that a fully self-consistent average is performed over all possible choices of cluster momenta. This removes the error that is introduced into the system by approximating the self-energy as a step function in $\mathbf{k}$ space for a given choice of cluster momenta. Consequently, the theory yields a fully continuous $\mathbf{k}$-space self-energy and spectral function for all cluster sizes. Impor-

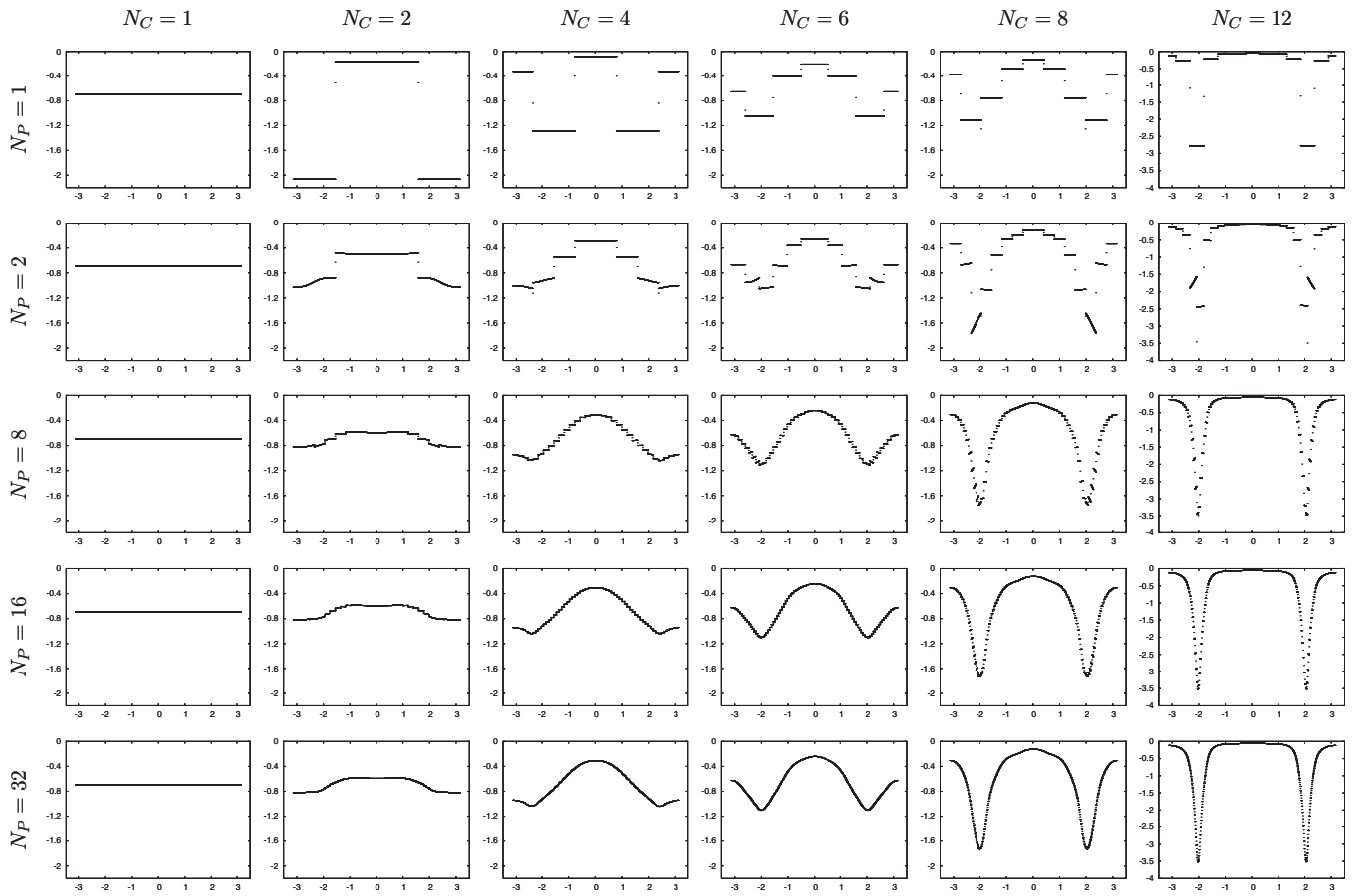

FIG. 6. Imaginary part of the self-energy as a function of **k** obtained using the NLCPA at an example energy of $E = \pm 3.0$. Results are shown for a selection of cluster sizes N_c (left to right) and number of phases included N_p (top to bottom). The single phase result is for the conventional $\phi_x = 0$ choice. With increasing N_p, observe the systematic convergence toward the correct self-energy for a given N_c. Also observe the convergence toward the exact (lattice) self-energy with increasing N_c.

tantly, this also means that the reformulation can be readily used to study SRO effects on Fermi surfaces of alloys, and could also be used as a basis for a theory of electronic transport[25] in disordered systems with SRO.

Another possible future area of applications is alloy energetics. Indeed, the NLCPA has recently been combined with density-functional theory for *ab initio* total-energy calculations. The resulting self-consistent-field (SCF)–KKR–NLCPA (Ref. 12) method can be straightforwardly adapted in analogy to the reformulation presented in this paper. While there are many alternative approaches aimed specifically at the calculation of alloy energetics (see Ref. 26 and references therein), an attractive feature of the NLCPA is that, like the single-site CPA, it could be used as a basis for a global *ab initio* mean-field theory of disorder which would describe concentration fluctuations in alloys[27] and also spin fluctuations in magnets at finite temperature.[28] Although the SCF-KKR-NLCPA can now be correctly implemented for any available cluster size, a practical limitation is the high computational cost for large cluster sizes due to the 2^{N_c} scaling (for a binary system), where N_c is the number of sites in the cluster. This needs to be addressed by implementing parallelization and importance sampling of the cluster disorder configurations. Finally, in addition to those research groups[6,10–13,22,25,29–33] performing calculations with the NLCPA, the work in this paper should be of significant interest to groups working with the DCA (Refs. 7 and 8) for the 2D Hubbard model.

ACKNOWLEDGMENTS

Research at LLNL was performed under the auspices of the U.S. Department of Energy by Lawrence Livermore National Laboratory under Contract No. DE-AC52-07NA27344. The ORNL part of the research was conducted at the Center for Nanophase Materials Sciences sponsored by the Division of Scientific User Facilities, U.S. Department of Energy.

APPENDIX: FIRST-PRINCIPLES ALGORITHM

Due to the analogy[2] between quantities in the tight-binding (TB) formalism and multiple-scattering KKR formalism, the TB formalism and algorithm presented in this paper can be carried over to KKR. As originally demonstrated in Ref. 9 for the conventional NLCPA, the key step is identifying the quantities in KKR which play the role of the self-energy in the TB framework.

First, the site-diagonal part of the self-energy Σ^{II} can be straightforwardly identified with the inverse of the effective

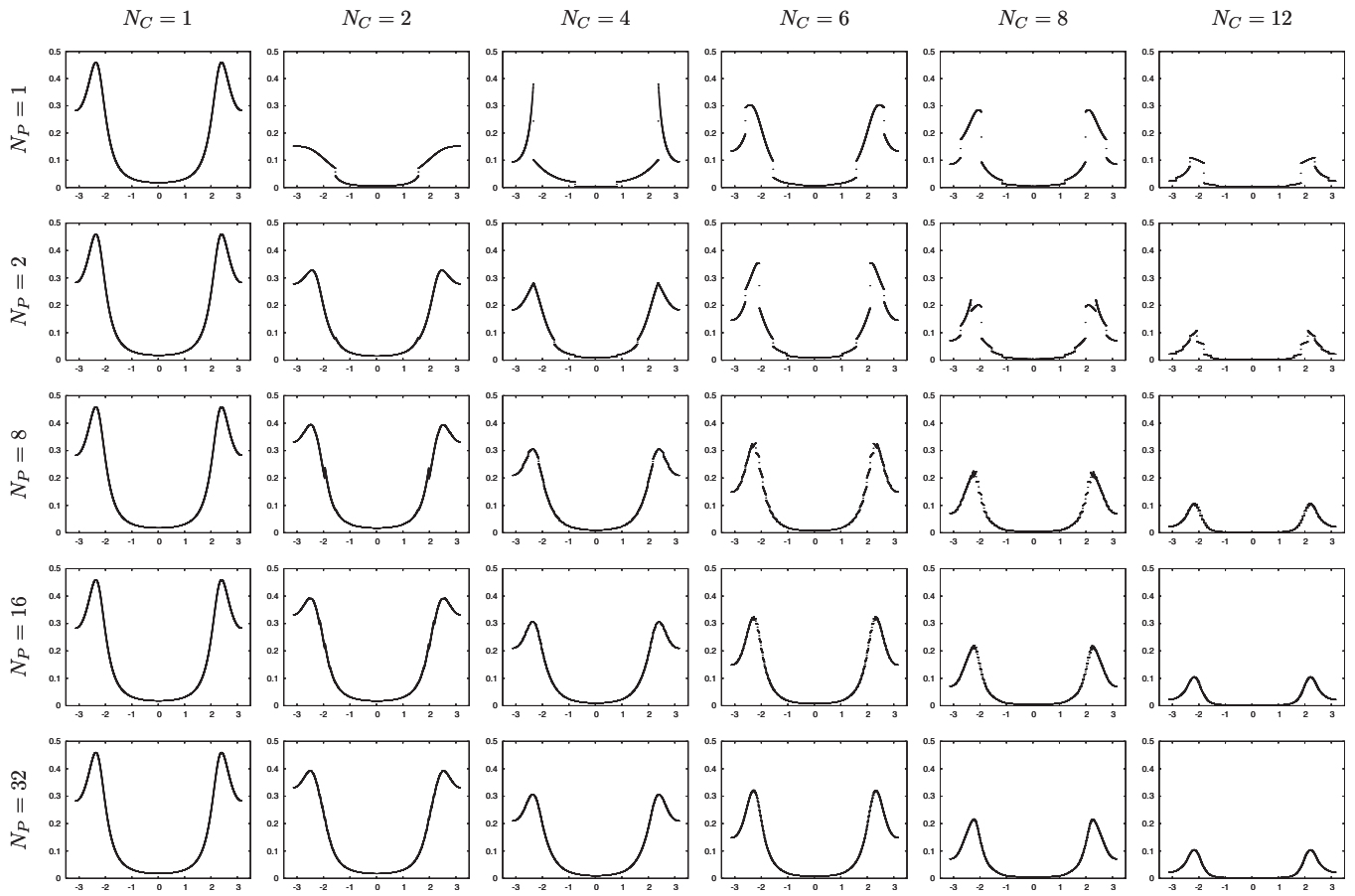

FIG. 7. Spectral function $A^B(\mathbf{k})$ obtained using the NLCPA at an example energy of $E = \pm 3.0$. Results are shown for a selection of cluster sizes N_c (left to right) and number of phases included N_p (top to bottom). The single phase result is for the conventional $\phi_x = 0$ choice. With increasing N_p, observe the systematic convergence toward the correct spectral function for a given N_c. Also observe the convergence toward the exact spectral function with increasing N_c.

t-matrix $\hat{\underline{t}}$ in KKR, which we denote as $\hat{\underline{m}}$. Second, since the off-diagonal part of the self-energy $\Sigma^{\overline{IJ}}$ can be viewed as providing effective medium (average) corrections to the pure hopping terms W^{IJ} within the TB framework, the off-diagonal terms Σ^{IJ} can be identified with effective corrections $\underline{\widehat{\delta G}}(\mathbf{R}_{IJ})$ to the free-space structure constants $\underline{G}(\mathbf{R}_{IJ})$ within KKR. Therefore the quantity playing the role of the self-energy, which we denote as $\hat{X}$, has matrix elements

$$\underline{\underline{\hat{X}}} = \begin{bmatrix} \underline{\hat{X}}^{11} & \underline{\hat{X}}^{12} & \underline{\hat{X}}^{13} & \cdots \\ \underline{\hat{X}}^{21} & \underline{\hat{X}}^{22} & \underline{\hat{X}}^{23} & \cdots \\ \underline{\hat{X}}^{31} & \underline{\hat{X}}^{32} & \underline{\hat{X}}^{33} & \ddots \end{bmatrix}$$

$$= \begin{bmatrix} \underline{\hat{m}} & -\underline{\widehat{\delta G}}(\mathbf{R}_{12}) & -\underline{\widehat{\delta G}}(\mathbf{R}_{13}) & \cdots \\ -\underline{\widehat{\delta G}}(\mathbf{R}_{21}) & \underline{\hat{m}} & -\underline{\widehat{\delta G}}(\mathbf{R}_{23}) & \cdots \\ -\underline{\widehat{\delta G}}(\mathbf{R}_{31}) & -\underline{\widehat{\delta G}}(\mathbf{R}_{32}) & \underline{\hat{m}} & \ddots \end{bmatrix}$$

$$\underline{\underline{\hat{X}}}(\mathbf{K}) = \begin{bmatrix} \underline{\hat{X}}(\mathbf{K}_1) & 0 & 0 & \cdots \\ 0 & \underline{\hat{X}}(\mathbf{K}_2) & 0 & \cdots \\ 0 & 0 & \underline{\hat{X}}(\mathbf{K}_3) & \ddots \end{bmatrix}$$

$$= \begin{bmatrix} \underline{\hat{m}} - \underline{\widehat{\delta G}}(\mathbf{K}_1) & 0 & 0 & \cdots \\ 0 & \underline{\hat{m}} - \underline{\widehat{\delta G}}(\mathbf{K}_2) & 0 & \cdots \\ 0 & 0 & \underline{\hat{m}} - \underline{\widehat{\delta G}}(\mathbf{K}_3) & \ddots \end{bmatrix}$$

in real and reciprocal spaces, respectively, where an underscore denotes a matrix in the angular momentum index. Note however that $\underline{\underline{\hat{\delta G}}}(\mathbf{R}_{IJ})$ takes account of nonlocal *scattering* correlations only. Nonlocal *charge* correlations can be described by combining the KKR-NLCPA with density-functional theory. This was recently carried out for the conventional KKR-NLCPA in Ref. 12 and provides a Madelung contribution to the total energy.

For completeness, the basic algorithm for the NLCPA reformulation is given below within KKR. All real-space matrices in the algorithm are matrices in the cluster site and angular momentum index only (denoted by a double under-

score) and all reciprocal-space matrices are diagonal.

(1) Begin with a guess for the (fully **k**-dependent) quantity $\hat{\underline{X}}(\mathbf{k})$; e.g., for the first iteration use the (**k**-independent) inverse of an average t matrix (ATA).

(2) Sample $\hat{\underline{X}}(\mathbf{k})$ at a selection of N_p sets of phases $\{\phi_d\}$ for each n, where $n=1,\ldots,N_c$, yielding the set $\{\hat{\underline{X}}(\mathbf{K}_n\{\phi_d\})\}$.

(3) Calculate the set of coarse-grained scattering path matrix elements

$$\hat{\underline{\tau}}(\mathbf{K}_n\{\phi_d\}) = \int_{\Omega_{\mathbf{K}_n\{\phi_d\}}} d\mathbf{k}[\hat{\underline{X}}(\mathbf{K}_n\{\phi_d\}) - \underline{G}(\mathbf{k})]^{-1}$$

for each n and each set $\{\phi_d\}$, where $\underline{G}(\mathbf{k})$ are the free-space structure constants.

(4) Calculate the **k**-space cavity function $\hat{\Delta}$ at the set of sample points via the equation

$$\hat{\underline{\Delta}}(\mathbf{K}_n\{\phi_d\}) = \hat{\underline{X}}(\mathbf{K}_n\{\phi_d\}) - [\hat{\underline{\tau}}(\mathbf{K}_n\{\phi_d\})]^{-1},$$

and convert to real space using the relation

$$\hat{\underline{\Delta}}^{IJ}\{\phi_d\} = \frac{1}{N_c}\sum_n \hat{\underline{\Delta}}(\mathbf{K}_n\{\phi_d\})e^{i\mathbf{K}_n\{\phi_d\}\cdot\mathbf{R}_{IJ}}.$$

(5) Calculate the impurity scattering path matrix

$$\underline{\tau}_\gamma\{\phi_d\} = (\underline{\underline{m}}_\gamma - \hat{\underline{\underline{\Delta}}}\{\phi_d\})^{-1}$$

for each set $\{\phi_d\}$, where $\underline{m}_\gamma$ is a cluster configuration of inverse t matrices.

(6) Sum over all configurations; i.e., calculate the configurationally averaged path matrix by summing over all impurity cluster configurations,

$$\hat{\underline{\tau}}^{IJ}\{\phi_d\} = \sum_\gamma P_\gamma \underline{\tau}_\gamma^{IJ}\{\phi_d\},$$

for each set $\{\phi_d\}$, where P_γ is the probability of configuration γ occurring.

(7) Calculate the new (phase-dependent) matrix elements $\hat{\underline{X}}_\phi^{IJ}\{\phi_d\}$ via the equation

$$\hat{\underline{\underline{X}}}_\phi\{\phi_d\} = \underline{\underline{\tau}}\{\phi_d\}^{-1} + \hat{\underline{\underline{\Delta}}}\{\phi_d\},$$

and convert to **k** space using the relation

$$\hat{\underline{X}}_\phi(\mathbf{K}_n\{\phi_d\}) = \sum_J \hat{\underline{X}}_\phi^{IJ}\{\phi_d\}e^{-i\mathbf{K}_n\{\phi_d\}\cdot\mathbf{R}_{IJ}}$$

for each n and set $\{\phi_d\}$.

(8) Sum over all phases; i.e., calculate the (fully **k**-dependent) path matrix

$$\hat{\underline{\tau}}(\mathbf{k}) = \int d\mathbf{K}_n[\hat{\underline{X}}_\phi(\mathbf{K}_n\{\phi_d\}) - \underline{G}(\mathbf{k})]^{-1},$$

where

$$\int d\mathbf{K}_n = \int_{K_{nx}(0)}^{K_{nx}(2\pi)} \int_{K_{ny}(0)}^{K_{ny}(2\pi)} \int_{K_{nz}(0)}^{K_{nz}(2\pi)} dK_{nx}(\phi_x)dK_{ny}(\phi_y)dK_{nz}(\phi_z)$$

in three dimensions, and the sum includes the appropriate set of $\hat{\underline{X}}_\phi(\mathbf{K}_n\{\phi_d\})$ associated with the point **k**.

(9) Calculate the new (fully **k**-dependent) quantity $\hat{\underline{X}}^{\text{new}}(\mathbf{k})$ via the equation

$$\hat{\underline{X}}^{\text{new}}(\mathbf{k}) = \hat{\underline{\tau}}(\mathbf{k})^{-1} + \underline{G}(\mathbf{k}).$$

(10) Compare $\hat{\underline{X}}^{\text{new}}(\mathbf{k})$ with the old $\hat{\underline{X}}(\mathbf{k})$ in step 1. If they are not equivalent within some prescribed tolerance, then repeat the algorithm from step 2 until convergence is achieved.

See Ref. 10 for full details of the quantities involved. The fully charge self-consistent total-energy formulation[12] can be similarly generalized.

[1] P. Soven, Phys. Rev. **156**, 809 (1967).
[2] A. Gonis, *Green Functions for Ordered and Disordered Systems*, Studies in Mathematical Physics Vol. 4 (North-Holland, Amsterdam, 1992).
[3] M. Tsukada, J. Phys. Soc. Jpn. **26**, 684 (1969).
[4] M. Tsukada, J. Phys. Soc. Jpn. **32**, 1475 (1972).
[5] F. Ducastelle, Solid State Phys. **7**, 1795 (1974).
[6] M. Jarrell and H. R. Krishnamurthy, Phys. Rev. B **63**, 125102 (2001).
[7] M. H. Hettler, A. N. Tahvildar-Zadeh, M. Jarrell, T. Pruschke, and H. R. Krishnamurthy, Phys. Rev. B **58**, R7475 (1998).
[8] M. H. Hettler, M. Mukherjee, M. Jarrell, and H. R. Krishnamurthy, Phys. Rev. B **61**, 12739 (2000).
[9] D. A. Rowlands, Ph.D. thesis, University of Warwick, 2004.
[10] D. A. Rowlands, J. B. Staunton, and B. L. Gyorffy, Phys. Rev. B **67**, 115109 (2003).
[11] D. A. Rowlands, J. B. Staunton, B. L. Gyorffy, E. Bruno, and B. Ginatempo, Phys. Rev. B **72**, 045101 (2005).
[12] D. A. Rowlands, A. Ernst, B. L. Gyorffy, and J. B. Staunton, Phys. Rev. B **73**, 165122 (2006).
[13] D. A. Rowlands, J. Phys.: Condens. Matter **18**, 3179 (2006).
[14] P. Dean, Rev. Mod. Phys. **44**, 127 (1972).
[15] A. Gonis and J. W. Garland, Phys. Rev. B **16**, 2424 (1977).
[16] To be more precise, "critical" here does not mean an abrupt cutoff point but rather a cluster size above which there is no observable difference in properties calculated from the corresponding Green's functions to within some appropriate tolerance. The differences will only become precisely zero by definition as $N_c \to \infty$.
[17] Similar observations have been found in DCA calculations for the 2D Hubbard model, attributed to "finite-size" effects. See, for example, Ref. 8, where it was noted the difference in transition temperature T_c obtained using the two choices of cluster

momenta is down to 5% for a 6×6 cluster; i.e., $N_{cr}\approx36$ for this system.

[18] A method for removing all discontinuities by performing a weighted average of the **k**-space Green's function over two different choices of cluster momenta was formulated in Ref. 29. The scheme is analytic, in contrast to interpolation methods used in the DCA (Ref. 34). Although non-self-consistent, the scheme can be viewed as taking initial steps toward the derivation of the present fully self-consistent formulation, which averages over all possible choices of cluster momenta.

[19] A. Bobbio, A. Horvath, M. Scarpa, and M. Telek, Perform. Eval. **54**, 1 (2003).

[20] G. Kotliar, S. Y. Savrasov, G. Palsson, and G. Biroli, Phys. Rev. Lett. **87**, 186401 (2001).

[21] T. A. Maier, M. Jarrell, T. Pruschke, and M. H. Hettler, Rev. Mod. Phys. **77**, 1027 (2005).

[22] R. Moradian, B. L. Gyorffy, and J. F. Annett, Phys. Rev. Lett. **89**, 287002 (2002).

[23] R. Moradian, Phys. Rev. B **70**, 205425 (2004).

[24] R. Moradian, J. Phys.: Condens. Matter **18**, 507 (2006).

[25] P. R. Tulip, J. B. Staunton, S. Lowitzer, D. Kodderitzsch, and H. Ebert, Phys. Rev. B **77**, 165116 (2008).

[26] A. V. Ruban and I. A. Abrikosov, Rep. Prog. Phys. **71**, 046501 (2008).

[27] B. L. Gyorffy and G. M. Stocks, Phys. Rev. Lett. **50**, 374 (1983).

[28] J. B. Staunton and B. L. Gyorffy, Phys. Rev. Lett. **69**, 371 (1992).

[29] G. M. Batt and D. A. Rowlands, J. Phys.: Condens. Matter **18**, 11031 (2006).

[30] D. A. Biava, S. Ghosh, D. D. Johnson, W. A. Shelton, and A. V. Smirnov, Phys. Rev. B **72**, 113105 (2005).

[31] S. Ghosh, D. A. Biava, W. A. Shelton, and D. D. Johnson, Phys. Rev. B **73**, 085106 (2006).

[32] P. R. Tulip, J. B. Staunton, D. A. Rowlands, B. L. Gyorffy, E. Bruno, and B. Ginatempo, Phys. Rev. B **73**, 205109 (2006).

[33] D. Ködderitzsch, H. Ebert, D. A. Rowlands, and A. Ernst, New J. Phys. **9**, 81 (2007).

[34] T. A. Maier, T. Pruschke, and M. Jarrell, Phys. Rev. B **66**, 075102 (2002).